Microfluidic Flow Cytometry

Sarah Duclos Ivetich, Stavros Stavrakis, and Andrew J. deMello

Abstract Flow cytometry is the most widely used method for the rapid enumeration of cells suspended in fluid media. Because of its quantitative and multiparametric nature and operational throughputs of up to 50,000 cells/s, flow cytometry is considered the gold standard method for identifying cells within heterogeneous populations. Unfortunately, conventional flow cytometers are costly, mechanically complex, consume large sample and reagent volumes (due to the need to use sheathing fluids), and require trained personnel for both operation and maintenance. To overcome these limitations, significant efforts have focused on miniaturizing and simplifying benchtop flow cytometers to realize microfluidic platforms able to sensitively assay cells in a high-throughput manner. In this chapter, we present the key features and characteristics of microfluidic-based flow cytometers. We then detail the various methods employed to manipulate and focus cells within flowing streams. This is followed by a discussion of contemporary optical detection systems and how these may be integrated within microfluidic platforms. We emphasize the significance and opportunities associated with imaging flow cytometry, detailing different imaging modes and how they may be used to enhance information content while maintaining high-throughput operation. To conclude, we explore the potential impact of emerging technologies, such as machine learning, in next-generation imaging flow cytometry.

Keywords Flow cytometry · Cell focusing · Microfluidics · Imaging · Fluorescence · Machine learning

S. D. Ivetich · S. Stavrakis (✉) · A. J. deMello (✉)
Institute for Chemical and Bioengineering, ETH Zürich, Zürich, Switzerland
e-mail: stavros.stavrakis@chem.ethz.ch; andrew.demello@chem.ethz.ch

D. A. Lamprou, E. Weaver (eds.), *Microfluidics in Pharmaceutical Sciences*,
AAPS Introductions in the Pharmaceutical Sciences 14,
https://doi.org/10.1007/978-3-031-60717-2_9

1 Conventional Flow Cytometry

Flow cytometry is the gold standard technique for enumerating cells, detecting biomarkers, and sorting cells from heterogeneous populations, with utility in a wide range of biological and clinical applications. Although the hemocytometer, a nineteenth-century innovation, provides a manual means of estimating cell concentrations, its limited analytical throughput and inability to extract specific cellular characteristics prompted the need for more advanced methodologies [66]. In the mid-1960s, Kamentsky et al. presented a rapid cell spectrophotometer using absorption as detection method [51]. In the late 1960s, Göhde and colleagues developed an impulse fluorimeter using a fluorescence microscope for the analysis of DNA in single cells [16]. This instrument formed the basis for the earliest commercial flow cytometers, developed in the late 1960s and early 1970s. As noted, modern flow cytometers are versatile and powerful tools for the quantitative and high-throughput characterization of cells at the single-cell level. In its most common embodiment, a flow cytometer utilizes hydrodynamic focusing to manipulate cells into a single file stream that passes through an optical detection volume. Sensitive and high-throughput optical analysis is normally achieved through the use of high-numerical aperture optics and photomultiplier tube (PMTs) detectors [38, 77]. As cells (or other micron-sized objects) pass through the detection volume, they can generate various optical signals, most notably forward scattered light (FSC), side scattered light (SSC), and fluorescence, which can then be used to assess cellular size, shape, morphology, granularity, and internal structure (Fig. 1).

The transferal and collection of optical signals at a photodetector is typically achieved using free-space optical components such as mirrors, lenses, and filters. The wavelength selectivity of a photodetector is most easily achieved by placing an optical filter in front of the detector, thus allowing only a user-defined range of wavelengths to be transmitted [23, 112]. While all flow cytometers are able to analyze both scattered light and fluorescence emission, fluorescence is most commonly used in biological applications. Here, a monochromatic laser is used to excite intrinsic or extrinsic fluorophores on or inside a cell. Fluorophores subsequently emit (red-shifted) fluorescence photons in an isotropic manner. These emitted photons are then discriminated from excitation photons using appropriate optics and detected using a PMT. Fluorescence detection is especially useful in identifying cell types based on surface marker expression, assaying DNA content, and assessing intracellular signaling [81, 95]. Multiparametric measurements of single cells enable the detailed characterization of cellular component distributions or variations in the expression of genes for fluorescent proteins. In this regard, access to multiple (fluorescence) detection channels is critical in allowing the investigation of complex cellular features [83].

Flow cytometers are able to operate at high analytical throughput, processing cells at rates up to 50,000 cells/s. This allows for the efficient analysis of large cellular populations and the detection of rare cells within complex media. Importantly, flow cytometry is non-destructive, enabling the recovery or selection of cells from heterogeneous populations if integrated with a sorting capability.

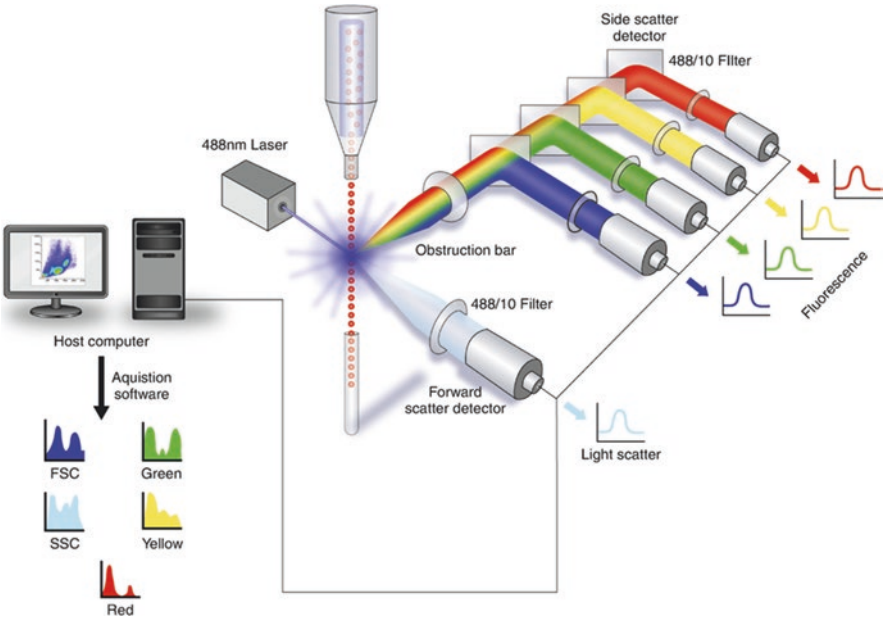

Fig. 1 Schematic illustrating the working principle of an optical flow cytometer. Sample containing cells or particles is injected into a sheath fluid at a slightly higher pressure than the sheath fluid. Hydrodynamic focusing creates a laminar sample flow where cells move in a single file within the sheath fluid. The sample stream is directed toward an optical detection volume. One or more laser sources are used to provide collimated excitation light, which is either absorbed (and subsequently re-emitted as fluorescence) or scattered by the cells as they move through the probe volume. Optical filters and/or dichroic mirrors are used to selectively transmit or block emitted fluorescence or scattered light. Photodetectors, normally photomultiplier tubes, capture these optical signals and convert them to electronic signals. Data processing/analysis is then used to simultaneously extract multiple parameters at the single-cell level. (Reprinted with permission from Hoogendoorn [43])

Fluorescence-activated cell sorters (FACS) integrate a sorting modality within a standard flow cytometer and enable the sorting of heterogeneous cell populations into pure sub-populations after their passage through the detection volume. In a typical embodiment, the cell stream is broken into small droplets that contain single cells. These droplets are electrostatically charged and then manipulated by a pair of electrically charged deflection plates. In theory, cells may be sorted at throughputs of between 10^4 and 10^5 cells/s, although practical constraints normally limit sorting rates to between 10^3 and 10^4 cells/s. This added capability makes flow cytometry a particularly versatile tool in biomedical research and clinical diagnostics, in applications such as immunology, hematology, cancer diagnostics, and drug discovery [63]. Indeed, flow cytometry has become indispensable in the diagnosis of blood cancers [35], the phenotyping of T cells [88], the detection of rare cells [30] and the rapid analysis of bacteria [75]. Unsurprisingly, flow cytometers generate enormous amounts of data, which are typically presented as multidimensional scatterplots or histograms.

Despite its central role in cellular analysis, flow cytometry is not without its limitations. Conventional flow cytometers are expensive, have large footprints (hindering their use outside of the laboratory), consume large volumes of sample and reagent, and require trained personnel for both operation and maintenance [106]. To address these issues, recent attention has focused on the development of microfluidic flow cytometers, with a view to realizing the sensitive and rapid analysis of single cells while minimizing sample/reagent volumes and instrumental footprints [83].

2 Microfluidic Flow Cytometry

As noted, microfluidic flow cytometers offer a number of significant features not accessible to conventional flow cytometers. These include the precise manipulation of micron-sized species particles in a sheathless manner [90], the ability to process sub-microliter sample and reagent volumes, and the direct integration with downstream analytical processing [106]. These benefits have ensured that microfluidic flow cytometers have emerged as innovative tools for cellular analysis in a range of applications [83].

Microfabrication techniques are fundamental in the creation of microfluidic flow cytometers. Of particular note is soft lithography [108]. Soft lithography is an umbrella term describing the molding of a soft material (such as an elastomeric polymer) by a lithographic master. Due to their simplicity and accessibility, soft lithographic methods have been used to fabricate microfluidic systems for a wide range of applications. The most common substrate material used in soft lithography is polydimethylsiloxane (PDMS). PDMS is biocompatible and possesses excellent optical, mechanical, and electrical properties [93]. Significantly, a range of detection modalities can be integrated or used with PDMS. For example, various optical components, such as air mirrors, air lenses, and optical fibers, can be integrated within microfluidic substrates [37]. As discussed, lenses and mirrors are used to focus and direct optical signals, and are essential components in flow cytometers [10, 87]. They improve the signal-to-noise ratio (SNR) associated with optical signals by reducing optical losses. Empty microchannels can be repurposed and tailored to accommodate optical fibers, enabling a facile connection between optical sources, samples, and detectors [37]. For example, Golden and co-workers integrated multiple optical fibers within a microfluidic flow cytometer, enabling the simultaneous detection of multiple parameters [26]. In a similar fashion, Mao et al. integrated four optical fibers within their microfluidic flow cytometer to link a single excitation light source with three optical detectors for FSC, SSC, and fluorescence detection [65].

The most obvious feature of a microfluidic device is its small size, which is critical for in-the-field or point-of-care use [21]. That said, true system portability relies on the integration and miniaturization of detectors (discussed below) and pumps. Membrane-based micromixers, microvalves, and micropumps are cost-effective

solutions for fluid manipulation [4]. These systems, typically made from PDMS, comprise two microfluidic layers; a pneumatic control layer and a fluid flow layer separated by an elastic membrane. This construct allows for controlled deflection of the control layer membrane against the fluidic layer, generating a peristaltic effect that propels fluid along the microchannel from inlet to outlet. Unfortunately, such components rely on external pneumatic actuation, which significantly impacts the instrumental footprint and limits device portability. Accordingly, the development of miniaturized pneumatic control systems for valve/pump operation is essential. In this regard, Chia et al. introduced an elastomeric thermal valve utilizing a heating electrode for control. This approach simplifies the external support architecture, but the use of high temperatures does pose a risk when processing biological species [12]. Alternatively, Takayama et al. presented an off-chip pneumatic control microvalve using inkjet printer needles as actuators. While interesting, the fixed position of the printer needle restricts flexibility in microvalve positioning within the microfluidic device [31].

Finally, electronically actuated micromixers, microvalves, and micropumps avoid the need for bulky external pneumatic control system and thus enhance the potential for out of laboratory use. Significantly, a range of microfabrication methods can be used to integrate electrodes into microfluidic devices and provide for electrical connection between on-chip components, such as active mixers, valves and pumps, and the outside world [91, 115].

3 Microfluidic Cell Focusing

Perhaps the most important part of the flow cytometry workflow is the focusing and alignment of cells. Ideally, all cells within a sample should be made to move along a defined trajectory that intersects with the optical probe volume. While traditional hydrodynamic focusing remains the most popular option for aligning and focusing cells, a number of alternate and "sheathless" strategies have been introduced [14]. These methods minimize sample and reagent waste, are easy to establish and reduce particle acceleration through the optical probe volume. As previously noted, efficient cell focusing is crucial in optimizing the performance of a microfluidic flow cytometer. The ideal focusing method should ensure that each cell moves along a fixed trajectory through the optical probe volume and that only one cell is present within this volume at any time. The efficiency of particle focusing techniques can be assessed by measuring optical signals originating from standard particles (of known size) as they transit the detection volume, which is typically reported as either a full width half maximum (FWHM) or coefficient of variation (CV) of the focused particle profile. We now discuss the two most commonly used focusing techniques: hydrodynamic focusing and sheathless focusing [104].

3.1 Hydrodynamic Focusing

Hydrodynamic focusing is an effective technique for cell focusing in microfluidic flow cytometers, taking advantage of laminar fluid flow to precisely position cells or particles within a narrow flowing stream [100]. The method involves "squeezing" a cell suspension (sample) flow within a sheath fluid to create a narrow, single-file stream of adjustable width. In this way, the sample stream velocity increases, and thins to maintain a consistent flow rate, while the sheathing streams decelerate and become wider. Hydrodynamic focusing in microfluidic channels is normally achieved through the utilization of sheath flows that flank a central sample stream [26] (Fig. 2a). Such schemes are versatile and compatible with a wide range of cell types and sizes, making them popular in microfluidic flow cytometry platforms [102]. It is important to recognize that hydrodynamic focusing can be implemented in either two or three dimensions, with the sheath fluid partially (laterally) or completely surrounding the sample stream. When using planar, single layer microfluidic systems, 2D focusing is used to direct the sample stream into a vertical element. Conversely, conventional flow cytometers employ 3D focusing. This significantly

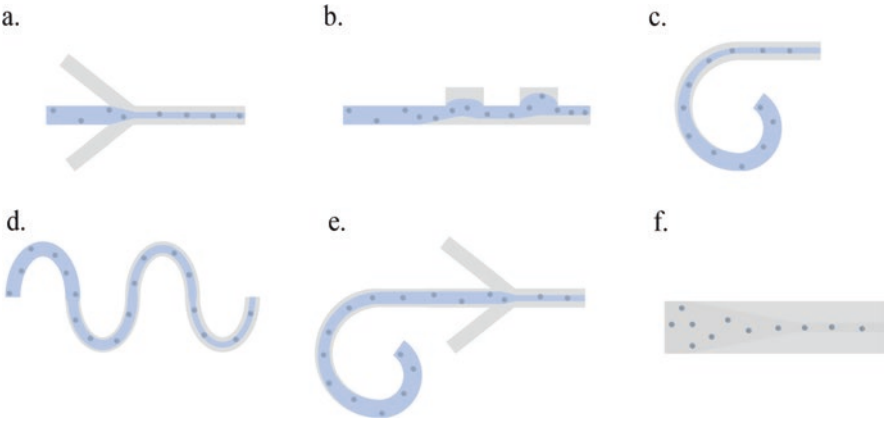

Fig. 2 Microfluidic cell focusing geometries. (**a**) 2D hydrodynamic flow focusing at a Y-Junction. Here a sheath flow is used to confine and focus cells in a microfluidic channel. (**b**) Inertial focusing using a multi-square contraction-expansion motif. Here, multiple contraction-expansion regions are employed within the channel to manipulate the flow and focus cells based on their size. (**c**) Inertial Dean flow focusing in spiral geometries. Inertial forces cause cells to migrate to specific equilibrium positions within the curved channel. Dean forces, generated by the concave structures in the spiral channel, facilitate particle focusing. (**d**) Inertial focusing within a serpentine channel. Serpentine curved channels with alternating turns can be easily parallelized, and by introducing asymmetry in the curvature (through different widths or radii of curvature), focusing similar to that in spiral channels can be achieved. (**e**) Combination of Dean and Y-junction sheath flows. This method combines the effects of Dean flows and sheath flows to achieve more precise and controlled focusing of cells within microfluidic channels. (**f**) Elasto-Inertial particle focusing within a rectangular straight channel. Elasto-inertial focusing utilizes a combination of elastic and inertial forces to focus particles or cells within a straight channel

enhances analytical sensitivity and ensures that cells move in a consistent manner through the optical probe volume [26]. However, as noted previously, conventional flow cytometers require excessive volumes of sheath fluid and necessitate the fabrication of multiple ports for sample and sheath fluid injection.

3.2 Inertial Focusing

The use of inertial forces to focus cells at high volumetric flow rates is advantageous since focusing is relatively insensitive to fluctuations in input flow rates. Inertial focusing is passive in nature, simply relying on control of flow-induced lift forces to both focus and space particles within defined trajectories. It's is simple to establish, has inherently high throughput, and does not require the use of sheath flows [29]. Significantly, the elimination of a sheath fluid enhances portability and reduces the cost of a flow cytometer. Inertial focusing can be realized in rectangular [46], square [13], triangular [54], or semicircular [53] cross section channels (Fig. 2b). However, the exact longitudinal placement of particles within a single sequential train requires additional forces since inertial focusing in the aforementioned structures yields multiple equilibrium positions across the channel cross section. Precise longitudinal control can be accomplished through the use of Dean-drag forces in curved [80, 105] (Fig. 2c), 2D [9] (Fig. 2d), or 3D spiral channels [8, 53], or via sheath flows (Fig. 2e). The integration of both sheath and Dean flows yields superior focusing and control of particle spacing compared to approaches that rely solely on Dean flows [57, 64]. An excellent diagnostic application of inertial focusing was reported by Ozkumur and co-workers in their CTC-iChip [79]. This platform aimed to efficiently capture and isolate circulating tumor cells (CTCs) from blood samples, utilizing inertial microfluidics to manipulate magnetically tagged cells into a (near) single file stream so that they can be precisely deflected and isolated using minimal magnetic force. The CTC-iChip device allowed for the isolation of rare CTCs from a confounding background of other blood cells, holding much promise for cancer diagnosis and monitoring. However, it should be noted that inertial focusing systems demand high flow rates and sometimes complex microchannel designs to ensure efficient focusing. This issue is recognized to be a bottleneck in imaging flow cytometry (iFC) due to the rapid signal processing requirements [42].

3.3 Viscoelastic Focusing

As noted, inertial focusing schemes allow for precise cell manipulations but require the use of relatively high volumetric flow rates. An alternative strategy involves leveraging the rheological properties of the carrier fluid to generate both inertial and elastic forces, which can be used to focus cells at lower volumetric flow rates [116]. Put simply, by tuning the rheological properties (and flow conditions) of

non-Newtonian fluids, cells and particles may be focused into single file streams at the channel centerline [58, 110, 114]. Significantly, viscoelastic fluids can be used to manipulate cells at flow rates as low as a few microliters per hour. When elastic lift forces are accompanied by inertial lift forces (elasto-inertial regimes) [59], effective focusing of cells and particles may be realized (Fig. 2f) at velocities as high as mL/s [42, 109, 113]. The interplay between elastic and inertial forces allows for precise manipulation and focusing across a wide range of flow rates, therefore expanding the potential applications of particle manipulation techniques.

4 Detection Systems for Microfluidic Flow Cytometers

Extraction of cellular information can be realized in a variety of ways, almost all of which are based on optical techniques. In the following sections, we describe of how light is made to interact with cells and how their responses are measured and recorded. Unsurprisingly, the choice of detection method has a significant impact on the overall design and structure of the microfluidic platform, noting that it is common for more than one detection technique to be used at the same time [101]. In addition, some detection methods may require the use of labels to probe cellular structure or composition, while others, such as electrical impedance, operate in a label-free manner. Finally, flow cytometers can be broadly categorized as being either "single point" or "imaging" in nature. Single point flow cytometers (spFCs) incorporate a single detection point (or volume) to analyze cells within a single file flow, whereas imaging flow cytometers (iFCs) combine the high-throughput capabilities of single-point flow cytometry with the imaging capabilities of an optical microscope.

4.1 Single Point Flow Cytometers

4.1.1 Optical Detection Systems

SpFCs incorporate a single optical detection volume to probe flowing cells in a sequential manner [28]. This approach, introduced previously, is employed in almost all commercial flow cytometers and has been adopted in a wide range of microfluidic flow cytometers. Several studies have reported powerful microfluidic spFCs, with the following studies showcasing some key advancements. For example, Xun et al. reported a sheathless microfluidic cytometer employing geometric confinement to focus white blood cells (WBCs), with both side scattered light and fluorescence detection capabilities [111]. Such an approach provided for low coincidence error rates, while its simple construction and sheath-free operation rendered it suitable for point-of-care use. Jiang et al. developed a microfluidic cytometer utilizing electrokinetically induced pressure-driven flow and dual-wavelength

fluorescence detection to simultaneously enumerate two different fluorescent particle populations, achieving a throughput of approximately 20–40 particles/s [49]. While the throughput is modest, such an approach effectively mitigates the drawbacks associated with pressure-based pumping methods. In addition, the use of two photodetectors significantly reduces both reagent and sample usage. Shi and coworkers developed a microfluidic platform for WBC detection using a four-part differential count, enabling the detection of lymphocytes, monocytes, neutrophils, and eosinophils [96]. Here, the selective staining of WBCs in blood samples was achieved through the application of three different fluorophores, with WBCs being detected by measuring fluorescence at wavelengths above 600 nm, and identification of subtypes being achieved by concurrent measurement of red and green fluorescence (between 520 and 550 nm). Significantly, data obtained from microfluidic cytometer were in close correspondence with data from conventional laboratory tests, while consuming only 5 μL of blood. In a related work, Simon et al. presented a microfluidic device that enabled simultaneous (multi-frequency) impedance and optical signal measurements for leukocyte differentiation in whole blood, with leukocyte subpopulation analysis achieved through the measurement of immunofluorescence signals from stained cells [97]. Importantly, the device was capable of not only identifying WBCs, but also platelets, erythrocytes, granulocytes, monocytes, and lymphocytes. However, no additional preparation steps, beyond diluting whole blood, were needed to perform a complete blood count. To address analytical throughput, Fan et al. reported a microfluidic device that incorporated 32 detection channels, 64 sheath flow channels, and a high refractive index microball lens array for high throughput multicolor fluorescence detection. Using such a system, the authors demonstrated a throughput of 358,400 cell/s [119].

Finally, it should be noted that in many microfluidic flow cytometers, optical components are located outside of the microfluidic device itself. While the use of (external) free-space optics can simplify device design, such systems tend to be costly and less well suited for in-the-field or point-of-care applications. Accordingly, a more cost-effective and flexible solution involves the integration of optical fibers or waveguides into the device [27, 65, 92]. Integration of these elements enables facile connection of the microfluidic system with external optical components and, as a result, reduces cost and enhances portability.

4.1.2 Impedance Detection Systems

In addition to optical detection systems, electrical detectors have long been used in Coulter counters to detect, enumerate, and size cells [2]. Such detectors can be easily integrated into microfluidic systems offering the possibility of label-free detection of cells in a high-throughput manner. While a number of microfluidic impedance cytometers have been demonstrated, they commonly employ co-planar electrodes, which can lead to measurement variations due to the generation of non-uniform electric fields [72, 118]. Such position-dependent impedance signals arise because cells or particles may follow different trajectories and thus interact differently with

electric fields within the detector. Accordingly, the implementation of particle focusing techniques, such as those described previously, becomes crucial in mitigating signal variations.

Impedance detection is the most popular electrical detection method in electrical flow cytometry. It relies on the measurement of the current flowing between two electrodes, with signals being dependent on the impedance of the particles flowing between them. Put simply, as cells move along a microchannel, they displace the surrounding electrolyte, and cause measurable fluctuations in electrical impedance. Importantly, impedance variations can be directly related to cellular properties such as size, volume, and dielectric constant. Accordingly, measurement of impedance variations offers insights into cell dimensions, shape, morphology, and physiological attributes (such as membrane integrity). This in turn allows discrimination of cells with similar geometry and size but different internal composition [39]. An early example of microfluidic impedance cytometry was presented by Karen et al. who employed two frequencies to differentiate between differently sized microbeads and various types of red blood cells [52]. Specifically, a low frequency signal was used as a reference, with a second frequency being used to differentiate between differently sized microbeads and intact, fixed, or lysed red blood cells. In related work, Chen et al. used impedance amplitude ratios and transit times to distinguish between different cell types [11]. Specifically, such an approach enabled a 93.7% success rate in distinguishing between osteoblasts and osteocytes, whereas differentiating between similarly sized wild-type and drug-resistant breast cancer cells was realized at a success rate of 70.2%. Interestingly, this type of detection method has been also used to distinguish neural stem cells and characterize two distinct tumor cell types [117]. Both aforementioned studies incorporate constriction channels (with a channel diameter to cell diameter ratio equal to or lower than one) to deform cells as they pass through the channel and ensure single-file cell flow. While the use of constriction channels is advantageous, for preventing current leakage during impedance measurements and introducing an additional variable for cell classification, the elongation length, they are susceptible to clogging. To address this issue, impedance-based cytometers comprising parallel-electrode configurations have been developed. Such formats improve reliability (by preventing channel blockage) and enhance versatility in cell classification, and typically incorporate one or more pairs of electrodes positioned along the top and bottom of a microchamber [22].

5 Microfluidic Imaging Flow Cytometers

The lack of imaging information afforded by single-point detection schemes is a significant limitation of conventional flow cytometers. Accordingly, there is a recognized need for platforms that combine the high-throughput capabilities of conventional flow cytometry with the imaging abilities associated with optical microscopy. Fortunately, in recent years, developments in high-speed optical imaging technologies have engendered significant improvements in both temporal and

spatial resolution, circumventing many of the technical issues associated with low camera frame rates and reduced sensor sensitivities [69]. We now describe some of the most important recent advances in iFC. For simplicity, we categorize such flow cytometers on the basis of the imaging method, namely those incorporating photodetectors and those integrating cameras; the main difference being that in photodetector-based systems, images are reconstructed from single point signals, whereas in camera-based systems, images are recorded without the need for any post-processing [98].

5.1 Camera-Based Imaging Flow Cytometers

The incorporation of a camera into a flow cytometer provides many benefits when compared to point-based detection schemes. That said, the ability to image cells at high throughput is far from simple. In this regard, mitigation of optical blurring is the primary challenge since cells are almost always moving at high linear velocities. The first commercial iFC, the ImageStream®, introduced by Amnis Corporation in 2005, addressed this issue by employing an epifluorescence excitation scheme and time delay and integration (TDI) cameras [6]. Such an approach enabled high-resolution multichannel imaging capabilities, but with a modest analytical throughput of less than 5000 cells/s (Fig. 3a). TDI imaging is a method that involves electronically panning the detector to effectively track object motion. In TDI, the sensor accumulates signal information from not just a single row of pixels at a time, but from multiple rows simultaneously, providing enhanced sensitivity. This accumulation helps in capturing a composite image of a moving object with reduced motion blur, as each row of pixels adds information about the object's position over time. By continuously shifting the accumulated charge from individual pixels, TDI compensates for the motion of the object being imaged, allowing for the detection of weak signals without the motion blur that is caused by increases in exposure time. Spectral decomposition enables the simultaneous acquisition of 12 images per cell [5].

Although the ImageStream® platform has shown its utility in various biological applications, including cell-cycle analysis and apoptosis detection [82] it is complex, bulky, expensive, consumes enormous volumes of sheath fluid, and requires trained personnel for operation and maintenance. Fortunately, the basic principles that underpin iFC are well suited to operation within microfluidic formats. For example, Di Carlo and co-workers developed a label-free, high-speed IFC platform integrating an inertial microfluidic device to analyze red blood cells and leukocytes at throughputs of approximately 28 million cells/s [46]. The sheathless device utilizes a single inlet, branching into 256 channels in which cells are positioned and spatially ordered by inertial forces. While the platform highlighted the potential of chip-based IFC, poor brightfield imaging resolution reduced its utility in morphological or multi-parametric imaging studies. To overcome this limitation, Holzner et al. developed an optofluidic flow cytometer that combines a refractive microlens

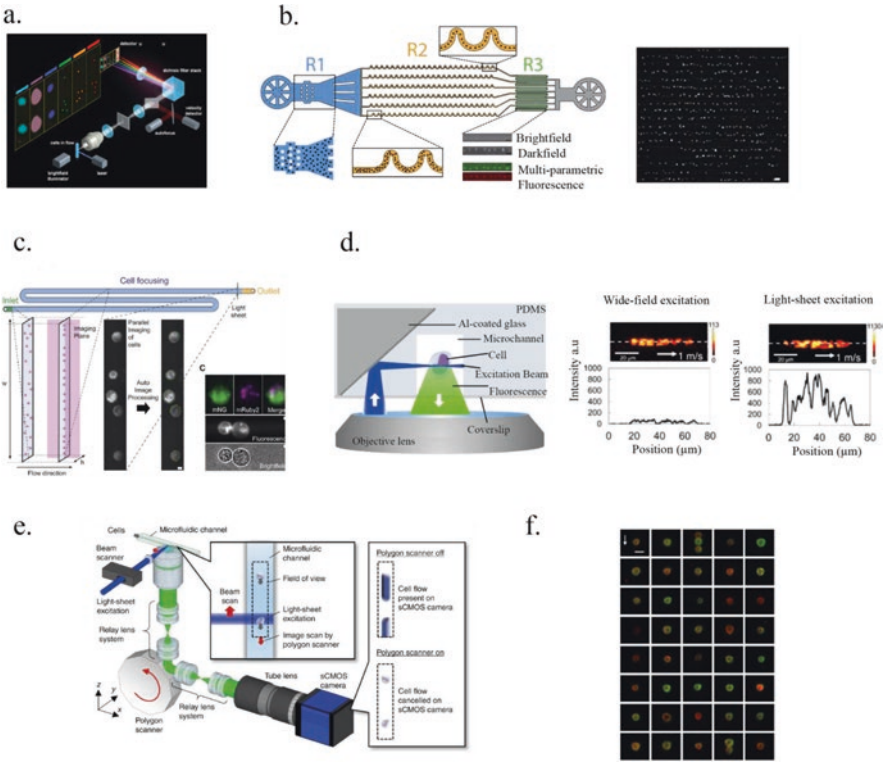

Fig. 3 Camera-based IFCs. (**a**) Schematic of the optical system within an ImageStream® flow cytometer. Cells labeled with fluorescent markers are hydrodynamically focused within the flow, and multiple laser lines are utilized to excite fluorescence. Using several imaging objectives with different magnification, brightfield, side scatter (SSC), and fluorescence images are captured and then transferred to a filter stack where each color is projected to a spatially discrete channel on the cameras. This method enables the collection of up to 10 fluorescence colors aligned spatially, so each probe is measured for intensity, morphology, and relative location to other probes. (Reproduced with permission from Cytek Corporation). (**b**) Schematic of a microfluidic platform for iFC based on inertial focusing and stroboscopic illumination. The system comprises an inlet port (blue), parallel channels for sheathless inertial cell focusing (orange), a detection area for multiparametric acquisition (green), and an outlet port for cell collection (gray). The grayscale image reports HL60 cells moving at a velocity of 0.35 m/s and using a stroboscopic pulse length of 10 μs. (Reprinted with permission from Rane et al. [85]. Copyright 2017 Cell Press). (**c**) Schematic of a microfluidic iFC based on elasto-inertial focusing and stroboscopic illumination. The platform integrates multi-color light sheet illumination, an elasto-inertial cell focusing system, a dual-color beam splitter, and a CMOS camera. Cells are imaged upstream of the outlet using a light sheet excitation beam, allowing the acquisition of multi-color and brightfield images. (Reprinted from Holzner et al. [41]. Copyright 2021 Elsevier). (**d**) An iFC plarform integrating a mirror on the side of a microfluidic channel to position a light sheet parallel to the imaging plane. Comparison of *Euglena gracilis* microalgae images acquired using wide-field and light-sheet excitation. (Reprinted with permission from Miura et al. [73]. Copyright 2018 OSA Publishing). (**e**) Virtual Freezing Fluorescence Imaging Flow Cytometry. Inset shows that VIFFI is able to generate blur-free images of cells that would otherwise be blurred. (Reprinted with permission from Mikami et al. [71]. Copyright 2018 Springer Nature). (**f**) Representative fluorescence images of HT-29 cells acquired by VIFFI. Green, EpCAM-FITC; red, PpIX; blue, CD45-PE; scale bar, 20 μm; arrow, flow direction (1 m. s^{-1}). (Reproduced from Matsumura et al. [67] with permission from the Royal Society of Chemistry)

array with an array of parallel microfluidic channels for imaging cells at throughputs of up to 50,000 cells/s [40]. Results demonstrated that the optofluidic platform can efficiently count and magnify cells up to four times achieving an improvement in imaging resolution. Alternatively, Schonbrun and co-workers reported a microfabricated device integrating diffractive microlenses for imaging cells at a throughput of 2275 cells/s using brightfield microscopy [94]. However, the limited focal range of these lenses have restricted their utility to brightfield imaging of cells with diameters less than 6 μm and at relatively low throughputs.

A universal issue faced when performing fluorescence microscopy is the trade-off that exists between signal acquisition time and image quality/brightness. Unsurprisingly, this issue is exacerbated when the sample under investigation is moving during the imaging process. A number of studies have attempted to lessen the impact of this trade-off. For example, Rane and co-workers reported an ultra-high throughput iFC platform incorporating inertial focusing for sheathless manipulation of cells and stroboscopic illumination for blur-free fluorescence imaging of cells moving at high linear velocities [85]. By controlling both the applied volumetric flow rate and the camera frame rate, the platform was capable of imaging cells at throughputs as high as 96,000 cells/s while demonstrating fluorescence imaging at throughputs in excess of 50,000 cells/s. Importantly, the method is multi-parametric in nature, providing for brightfield, darkfield, and multi-color fluorescence imaging (Fig. 3b). Based on these capabilities, the platform was used to perform both high-throughput cell cycle and apoptosis studies. Whilst this approach afforded high-throughput operation, image resolution was poor. To address this issue, the same group subsequently reported a related microfluidic platform for high-throughput imaging of cells with (near to) diffraction limited imaging resolution [41]. To engender acquisition rates in excess of 60,000 cells/s (fluorescence) and 400,000 cells/s (brightfield), the authors combined stroboscopic illumination with elasto-inertial cell focusing, demonstrating enhanced control of both cell velocities and trajectories within the detection probe volume (Fig. 3c). Critically, this innovation enabled high-throughput investigations of phase-separated sub-cellular components and the screening of rare events at the sub-cellular level. In related studies, Miura and colleagues reported a light-sheet fluorescence IFC based on integrated micromirrors [73]. Here light sheet excitation parallel to the imaging plane is used to increase excitation efficiencies by an order of magnitude compared to conventional wide-field excitation approaches. Specifically, the excitation beam was strobed at a rate that matched the average cellular velocity (approximately 1 m/s), yielding an extrapolated maximum throughput of 10,000 cells/s (Fig. 3d).

An alternative method able to capture images of cells moving at high speed is Virtual Freezing Fluorescence Imaging Flow Cytometry (VIFFI), developed by Mikami and co-workers (Fig. 3e). VIFFI is an optomechanical imaging method that enables high-throughput acquisition of high-quality cell images by "virtually" freezing the motion of rapidly moving cells on a CMOS image sensor, effectively increasing exposure times by up to three orders of magnitude [71]. VIFFI has been used to perform rare cell detection of HT-29 cells spiked into peripheral blood mononuclear cell suspensions at rates of approximately 750 cells/s [67] (Fig. 3f).

5.2 *Photodetector-Based Imaging Flow Cytometers*

An excellent example of a PMT-based iFC was reported by Goda and associates, who developed an ultrafast and continuous imaging method known as STEAM. STEAM employs a detector array in conjunction with optoelectronic image-encoding and decoding techniques, to allow for high-throughput image-based screening at speeds approaching 100,000 cells/s [24]. The cytometer was used to identify rare mammalian cells (MCF7 cells tagged with 1 μm metal beads linked to specific antibodies) within blood samples. The method demonstrated exceptional sensitivity and was capable of detecting a single labeled MCF7 cell in the presence of a million WBCs, with a false-positive rate two orders of magnitude lower than that observed when using conventional fluorescence flow cytometry. However, it should be noted that this brightfield imaging method utilizes relatively long excitation wavelengths. Furthermore, and in a similar manner to the classical optical imaging modalities, the image quality of STEAM, characterized by image resolution and image contrast, is still compromised by the high imaging speed. Consequently, the practical application of STEAM has mainly focused on high-speed screening of target cells labeled with contrast agents [25]. To address these challenges, Tsia and colleagues introduced an innovative imaging technique known as asymmetric-detection time-stretch optical microscopy (ATOM) (Fig. 4a) [107]. ATOM excels at capturing label-free images with high contrast and sub-cellular resolution, and even at flow velocities in excess of 10 m/s. Unsurprisingly, the imaging throughput of ATOM is exceptionally high, exceeding 100,000 cells/s for consistently spaced cell streams [107]. Unlike conventional time-stretch imaging, which relies on all-optical image encoding and retrieval via ultrafast broadband laser pulses, ATOM enhances imaging performance by intensifying the image contrast of unlabeled or unstained cells. Interestingly, the same researchers have since applied ATOM to high-throughput screening and classification of phytoplankton based on variations in intracellular texture and morphology (Fig. 4a) [56].

Several recent reports have provided alternative solutions to the challenge of cellular imaging at high speeds. Notably, Diebold et al. developed an imaging technique that achieves real-time pixel readout rates significantly higher than those of traditional cameras, by mapping images into the radiofrequency domain using digitally synthesized optical fields [15] (Fig. 4b *left panel*). Such an approach, christened fluorescence imaging using radiofrequency-tagged emission or FIRE, allows for blur-free fluorescence imaging of cells moving at a speed of 1 m/s, resulting in an analytical throughput of 50,000 cells/s (Fig. 4b *right panel*). While this technique showcases the potential of high-speed fluorescence imaging, its practical use is limited by the complexity of the optical detection system, and its low sensitivity. In a related work, Goda and co-workers reported a frequency-division multiplexing confocal fluorescence microscope capable of imaging at frame rates of up to 16,000 frames/s [70]. This system showcased its utility in biomedical applications, including 3D confocal fluorescence imaging of motile microalgal cells and 2D confocal fluorescence IFC of white blood and microalgal cells at flow rates of up to 2 m/s. Using a simpler optical set up, Han et al. used a spatial-temporal transformation (using mathematical algorithms and a specially designed spatial filter) to furnish a

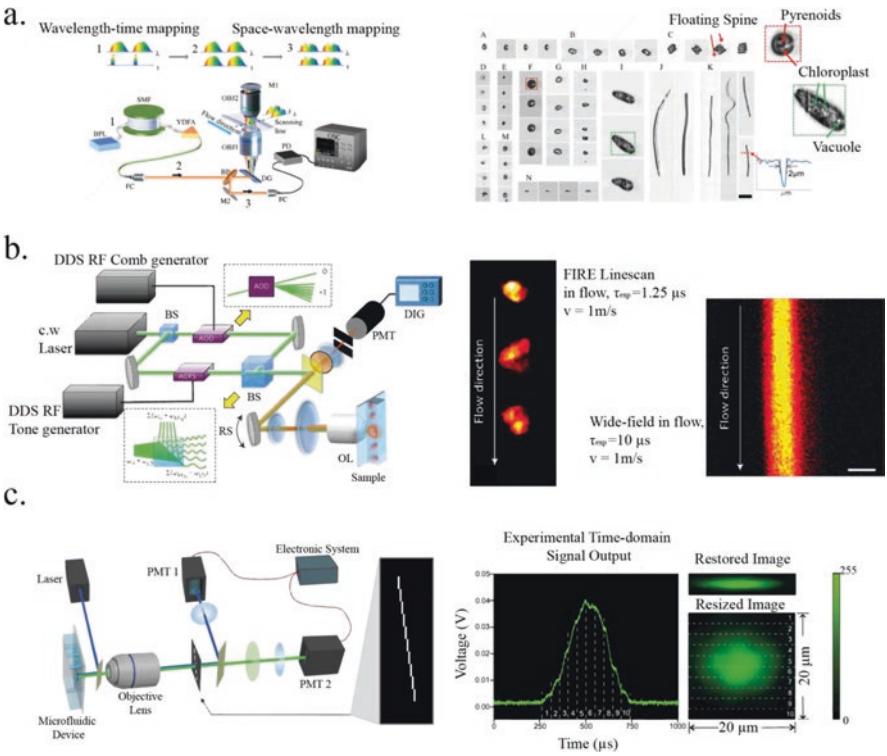

Fig. 4 Photodetector-based iFCs. (**a**) Schematic of an optofluidic time-stretch imaging system for iFC. Reconstructed images from a time stretch experiment of phytoplankton cells are shown on the right-hand side. (Reprinted with permission from [56] Copyright 2016 Optical Society of America). (**b**) Illustration depicting how FIRE may be used for blur-free fluorescence imaging of cells. Representative FIRE images of cells moving at a velocity of 1 m/s captured with a 10 µs exposure and images of individual cells recorded with an EMCCD flowing at the same velocity are shown on the right-hand side. Scale bar: 10 µm. (Reprinted with permission from [15]. Copyright 2013 Springer Nature). (**c**) Schematic of an iFC system equipped with a spatial filter. Time-domain PMT output signal, alongside the corresponding restored and resized fluorescence image, with the latter depicting the actual size of the cell are shown on the right-hand side. (Reprinted with permission from [33]. Copyright 2013 Springer Nature)

conventional flow cytometer with imaging capabilities (Fig. 4c) [33]. Using PMT detectors, high quality fluorescence and scattering images of rapidly moving cells could be obtained at throughput of approximately 1000 cells/s.

6 Three-Dimensional Imaging Flow Cytometry Via Light-Sheet Fluorescence Microscopy

A key limitation associated with conventional iFCs is that, regardless of the detection methodology employed, only two-dimensional (2D) cell images are obtained. While highly useful in a range of clinical applications, the ability to extract

three-dimensional (3D) images of single cells can often be critical in cell phenotyping studies, where sub-cellular components are often distributed throughout the entire cell volume. For example, if a fluorescent structure is observed at the center of a cell when performing conventional (2D) imaging, its true location (for example, in the membrane, cytosol, and nucleus) remains ambiguous. Accordingly, when performing internalization measurements, co-localization studies, and spot counting, only 3D images can provide a complete and accurate assessment of organelle location and morphology [45].

Light-Sheet Fluorescence Microscopy (LSFM) is an imaging technique that provides high-resolution, 3D images of biological species. Unlike traditional microscopy, LSFM employs a thin sheet of laser light to illuminate the sample. This thin sheet of light is oriented orthogonally to the imaging plane, creating a well-defined "light sheet." Selective plane illumination microscopy (SPIM) is a light-sheet microscopic technique that uses a focused light sheet to illuminate the specimen from the side [99]. This enables continuous imaging of the illuminated plane while capturing sequential images as the sample traverses through the plane. By either moving the sample or the light sheet through the sample, multiple two-dimensional images can be acquired at various depths. Subsequently, these images can be combined to reconstruct a high-resolution, three-dimensional image of entire biological species. Unsurprisingly, light-sheet microscopy has become an increasingly popular imaging technique due to its ability to provide excellent resolution images at high penetration depths.

Simultaneous cell counting and visualization of fluorescently labeled subcellular mitochondrial networks in HeLa cells have been achieved using light sheet-based iFC [86] (Fig. 5a). This system images species flowing through a PDMS microfluidic channel, allowing for single-shot scanning of cells moving at flow rates between 100 and 1000 nl/min. Interestingly, the microfluidic device was oriented at 120° from the excitation arm to ensure that scattered light does not enter the detector and thus enhances signal-to-noise ratios. In related work, Han and co-workers reported a high-throughput 3D iFC imager based on optical sectioning microscopy [34] (Fig. 5b). Here, orthogonal light-sheet scanning illumination was combined with spatiotemporal transformation detection to generate 3D cell images from single-pixel photodetector readouts. Specifically, the approach allowed the capture of both 3D fluorescence and label-free side-scattering images of single cells moving at a velocity of 0.2 m/s, corresponding to a throughput of approximately 500 cells/s, with a spatial resolution of less than 1 micron in all dimensions. Moreover, Ugawa et al. developed a parallel high-throughput 3D-iFC technique, based on light-sheet microscopy [103] (Fig. 5c). This method enables fast, parallel optofluidic scanning of cells by performing 1D acoustofluidic focusing of multiple cells under wide-field light-sheet microscopy with a single objective lens. Significantly, the approach allows for multicolor 3D imaging in flow and with an analytical throughput exceeding 2000 cells/s. Additionally, it facilitates large-scale 3D-morphology-based flow cytometric analysis of populations in excess of 10^5 cells. Finally, it should be noted that subcellular structures can be imaged at high throughput, thereby providing valuable cellular information that would often be overlooked when using traditional 2D-imaging cytometry techniques.

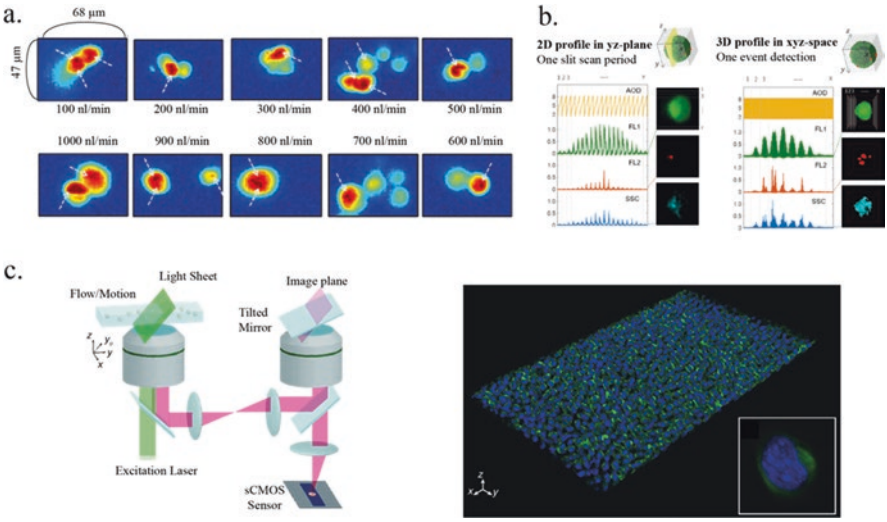

Fig. 5 Three-dimensional imaging flow cytometry. (**a**) Images of HeLa cells acquired at variable flow rates and a frame rate of 300 frames/s obtained using light sheet-based iFC. (Reprinted with permission from Regmi et al. [86]. Copyright 2014 AIP Publishing). (**b**) Illustration of how multiple scans can be used to produce a 2D profile in the *yz* plane as an object moves along the y-axis. Each section, separated by dotted lines, corresponds to the light intensity of one row in the 2D image stack. When an object completely traverses the spatial filter, the time-domain signal contains the complete information of the 3D profile in *xyz* space. (Reprinted from Han et al. [34]. Copyright 2019 Optica Publishing Group). (**c**) Schematic of the optical construction of a parallel 3D-iFC, featuring a remote objective (on the right-hand side) combined with a tilted mirror to transform oblique plane images into the lateral plane. The resulting converted image is projected onto a CMOS sensor. A 3D reconstructed image derived from high-throughput imaging of K562 cells deposited in a glass-bottomed well. The green and blue colors represent CFSE and DAPI fluorescence, respectively, with a close-up of a single cell in the bottom right. (Reprinted with permission from Ugawa and Ota [103]. Copyright 2022 Wiley-VCH GmbH)

7 Machine-Learning Assisted Imaging Flow Cytometry

IFC has been shown to be a powerful technology for image-based analyses of non-adherent cells at high throughput. It enables comprehensive analysis and in-depth imaging of each cell within a large population and allows the extraction of morphological profiles in a direct manner. Interestingly, traditional data analysis methods in flow cytometry normally rely on manual gating, a process whereby the user manually defines regions of interest within data plots to identify unique sub-populations of cells [61]. While this approach has its merits and uses, it comes with several limitations. Most notably, manual gating relies on subjective judgment to define or identify sub-populations. In addition, as datasets grow in size, manual analysis becomes time-consuming and impractical [48]. Indeed, iFC experiments almost always contain enormous amount of imaging data, and thus manual data analysis/processing is far from simple. Accordingly, the use of artificial intelligence (AI) and machine

learning (ML) algorithms to process and analyze iFC data is both needed and has the potential to transform the utility of iFC in a range of biological and clinical applications.

Unsurprisingly, ML algorithms are already being used to good effect in iFC and have been shown to provide more objective, consistent, and precise information [84]. In simple terms, machine learning is a branch of AI that uses algorithms and statistical models to learn from and make predictions or decisions based on previously recorded data. Unlike traditional programming methods, where explicit instructions are used to solve a problem, ML systems are designed to learn and improve their performance over time through the analysis of large datasets. Such a learning process involves the identification of patterns, relationships, and trends within datasets, which can then be applied to new and unseen data to make informed predictions or decisions [7]. With the rapid development of deep learning, a subfield of ML, the emergence of convolutional neural networks (CNNs) has revolutionized the field by offering a highly effective means to address complex learning tasks. Neural networks (NNs) are machine learning algorithms, inspired by the structure and function of biological neural circuits (populations of neurons interconnected by synapses), consisting of interconnected nodes (artificial neurons) organized into layers [1]. The input layer receives data, which is then processed through one or more hidden layers, with the output layer finally producing a prediction or classification. During training, NNs learn from data by adjusting the weights of connections between neurons, optimizing their ability to make accurate predictions or classifications for various tasks, including image analysis.

In the context of iFC, ML algorithms can be trained to automatically recognize and classify cell populations, detect anomalies, or extract valuable insights from complex multidimensional datasets, ultimately enhancing the efficiency and accuracy of the data analysis process. A generic workflow involves imaging cells of interest as they move through the detection volume of the flow cytometer. The detected image is then processed (ideally in real time) using a moving-object detection algorithm. This allows cells to be tracked and identified. Gathered images are segmented into individual pixels, creating a grayscale pattern that represents the detected cells against the background. This pattern is then analyzed and processed further to identify and track the cells of interest within the flow. Once completed, identification through ML can occur [62]. A particularly important clinical application of ML is in diagnostics (Fig. 6a). Cell-based diagnostic methods traditionally rely on the measurement of signals derived from specific biomarkers. These biomarkers could be proteins, DNA or RNA fragments, or other cellular components indicative of certain diseases or physiological states. However, in multiplexed assays, where multiple markers must be assessed simultaneously, the challenge often lies in the manual comparison and analysis of these various markers. This process involves examining multiple signals within a single sample, requiring time-consuming manual analysis and specialized software tools for interpretation. Interestingly, recent studies indicate that label-free imaging methods (e.g., bright-field and darkfield imaging) may be excellent substitutes for fluorescence. However, efficient extraction of phenotypical data requires complex image analysis. Classical

image analysis pipelines use predefined features as machine classifiers, which limits accuracy. In contrast, deep neural networks offer enhanced flexibility and improved accuracy by autonomously learning relevant patterns from extensive datasets. Their strength lies in their ability to automatically extract hierarchical and abstract features from raw data, allowing them to discern complex patterns that might be challenging for other algorithms or manual analysis.

CNNs are increasingly being used for single cell analysis and classification. For example, Meng et al. achieved high-accuracy identification of various cell types, including THP1, MCF7, MB231, and PBMC, using label-free imaging [68]. In another study, Göröcs and co-workers used phase-contrast color image reconstruction techniques to detect plankton in natural water samples (Fig. 6b), demonstrating the versatility of CNNs in image-based identification tasks within environmental contexts [32]. In addition, Eulenberg et al. successfully differentiated different phases of the Jurkat cell cycle, achieving a global accuracy of around 98.73% (Fig. 6c), underscoring the efficacy of CNNs in precise cell cycle stage recognition [20].

The integration of AI with cellular screening also has the potential to revolutionize the way we analyze and understand cells and tissues, leading to new discoveries and improvements in healthcare [55]. The analysis of cell morphology holds immense potential for discerning various cell types, states, and disease markers, opening up the field of blood-based diagnostics. In this regard, brightfield and darkfield iFC are emerging as powerful tools for classifying WBC types [60, 74] (Fig. 6d), and aiding in acute lymphoblastic leukemia diagnostics via residual CNN architectures [18]. Furthermore, morphology-based identification has proven

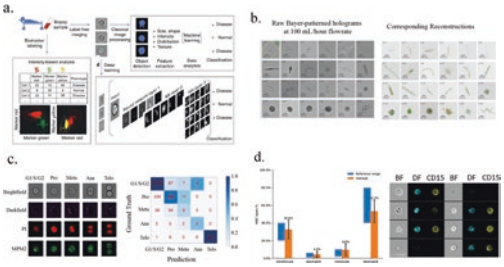

Fig. 6 Machine Learning Microfluidic Flow Cytometry. (**a**) Comparison of high-throughput cell-based diagnostic workflows based on either conventional or AI-aided workflows. (Reprinted with pression from Doan and Carpenter [17] Copyright 2019 Springer Nature). (**b**) Phase-contrast color image reconstruction techniques can be employed to detect and identify plankton in natural water samples. (Reprinted with permission from Göröcs et al. [32]. Copyright 2018 Springer Nature). (**c**) Representative images depicting cell cycle stages captured via brightfield, darkfield, and fluorescence imaging alongside "confusion matrices" demonstrating deep learning classification for these stages. (Reprinted with permission from Eulenberg et al. [20]. Copyright 2017 Springer Nature). (**d**) Comparison of average WBCs counts from 85 unstained blood donors with the WBC count range being obtained from images collected via iFC. (Reprinted with permission from Nassar et al. [74]. Copyright 2019 International Society for Advancement of Cytometry)

valuable in differentiating aggregated platelets from single platelets and WBCs, exhibiting high specificity and sensitivity [50]. Additionally, Doan et al. utilized iFC and deep learning to distinguish clinically relevant red blood cell morphologies associated with cell storage lesions [19]. The application of deep learning to iFC data shows immense promise for various clinical image classification tasks [89]. Finally, portable iFC has been integrated with CNNs to perform label free morphology-based diagnosis of cancer cells, in diseases such as Sézary syndrome [78].

Recently, Goda and co-workers demonstrated a real-time cell sorting instrument, combining high-throughput microscopy and real-time decision-making using a deep CNN thus enabling "intelligent image-activated cell sorting" [76]. This system involves a collection of individually complex operations such as 3D hydrodynamic focusing supplemented with acoustic focusing on a glass microfluidic chip, frequency-division multiplexed microscopy, a dual-membrane piezo push-pull cell sorter, and deep-learning-based image analysis for real-time sorting. The power of this approach was demonstrated by showcasing the sorting of microalgal and blood cells on the basis of subcellular protein localization and intercellular interactions. The same research group recently reported a modified version of this setup, utilizing a distinct imaging approach known as VIFFI [47].

In conclusion, advancements in both ML software and iFC hardware continue apace and will undoubtedly impact cell morphology analysis in clinical diagnostics, allowing for more accurate and faster classification with minimal human intervention.

8 Conclusions and Future Directions

While flow cytometry is undeniably an established and ubiquitous experimental tool in cellular analysis, we hope that the current discussion has highlighted that the technology set continues to develop apace. In particular, the adoption of microfluidic formats has begun to transform both analytical throughput (cells analyzed per unit time) and accessible information content. The transition from conventional formats to chip-based systems has proved to be both simple and empowering. For example, the adoption of chip-based flow cytometers ensures that integration with both up-stream and downstream functional components is simple. In addition, and as previously discussed, the implementation of microfluidic formats enables cell focusing (an essential component of the flow cytometry workflow) to be performed in a sheathless manner, through the use of inertial and viscoelastic forces. This simple modification engenders enormous enhancements in analytical throughput, minimizes sample and reagent consumption, and provides for exceptional control over cellular trajectories. Finally, it should also be remembered that the use of planar, chip-based formats ensures that a variety of optical (and electrical) detection schemes can be integrated with ease, providing for multiparametric analysis.

More excitingly, the adoption of microfluidic platforms has catalyzed the rapid development of iFC . As discussed, iFCs combine the high-throughput capabilities

of conventional flow cytometry with the imaging abilities associated with optical microscopy and enable high-throughput and high-information content analyses of heterogeneous cellular populations. While iFCS is a relatively nascent technology, it has already demonstrated extensive utility in cell biology and clinical diagnostics. Indeed, iFC is expected to make significant contributions to large-scale multiparametric cell analysis, leading to a deeper understanding of cellular behavior in the context of a certain disease. Put simply, in disease diagnostics, there is a recognized need for simple imaging methods able to classify cells without relying on the pathologist's objectivity. For example, the early diagnosis of cancer is a key determinant of patient outcome. Hematological malignancies manifest themselves in the blood and are therefore amenable to blood-based diagnostics. Traditionally, such diagnostic procedures rely on manual microscopical evaluation of blood cell morphology and suffer from subjectivity, limited throughput, and low sensitivity. The integration of iFC and ML can be used for morphology-based diagnosis of hematological malignancies, with identified blood cell sub-populations correlated with a specific disease state being used to train convolutional neural networks and create predictive models able to classify individual cells (as being healthy or diseased) [78]. Such an approach circumvents the challenges involved in defining molecular diagnostic markers and resurges morphology-based diagnosis of diseases through automated, efficient, rapid, and economic workflows.

While much progress is being made in "intelligent" flow cytometry, it should be remembered that the ability to collect and analyze extremely large numbers of (high-resolution) cell images is key to classifying diverse cell profiles without the need for predefined disease markers. Sophisticated deep learning models (particularly those tailored for object image recognition) can be used to enhance classification accuracy, but large datasets are normally needed to train such classifiers [36]. This presents numerous challenges. First, constructing labeled image datasets requires substantial input from clinicians so as to ensure accurate labeling aligns with morphological features. Second, such manual annotation becomes a time-consuming bottleneck in the IFC workflow due to the vast volume of data involved. To address this challenge, multiple instance learning, an extension of supervised learning, can be employed. In multiple-instance learning, disease annotations (e.g., "healthy" or "diseased") are assigned to a group of observations rather than individual observations. Multiple-instance learning is particularly appealing for biomedical image analysis, since clinical annotations characterize groups of observations. Interestingly, multiple-instance learning has already been successfully applied to cancer detection in histopathology imaging [44], where only the whole slide-level information is provided, as well as in the analysis of proteomic profiles of cell sub-populations associated with disease status [3].

To conclude, it is evident that the transition from conventional (capillary-based) formats to chip-based microfluidic formats has transformed both the performance and applicability of flow cytometry in a range of biological and clinical problems. Today, flow cytometers need not be expensive, complex, and large-footprint instruments that must be housed in central facilities and operated by trained personnel, but rather can be cost effective, portable, parallelized tools that can be implemented

in a variety of out-of-lab environments and provide high-quality biological information from complex cellular samples.

9 Multiple Choice Questions

1. Which of the following is true for flow cytometers that incorporate sheath fluid?

   A. The pressure in the sample fluid is higher than in the sheath fluid.
   B. The pressure in the sample fluid is lower than in the sheath fluid.
   C. The pressure in the sample fluid is equal to that in the sheath fluid.
   D. The lowered sample pressure ensures a single file flow of cells.

2. What is a key challenge associated with microfluidic flow cytometry?

   A. Sample throughput is limited.
   B. Integrating multiple detection methods is difficult.
   C. Microfluidic formats are incompatible with fluorescence detection schemes.
   D. The high costs associated with device fabrication.

3. What is a current challenge associated with microfluidic imaging flow cytometry?

   A. Poor compatibility of microfluidic devices with fluorescence imaging.
   B. Difficulty in performing real-time imaging when operating at high throughput.
   C. Difficulty in analyzing rare cells in a heterogeneous population.
   D. Lower sensitivities when compared to traditional flow cytometry.

4. Why does the use of a microfluidic platform enhance imaging accuracy in imaging flow cytometry?

   A. Cells can be manipulated more easily than in conventional systems.
   B. Sample viscosity is increased.
   C. Imaging speed is reduced.
   D. Optical resolution is improved.

5. What is meant by “gating” in flow cytometry?

   A. The process by which cells are introduced into the flow cytometer.
   B. The process by which cells are isolated within the optical detection volume.
   C. An electronic window that separates sub-populations of cells within a larger population.
   D. The process by which cells are delivered to different outlets in a flow cytometer.

10 Answers

1. A
2. B
3. B
4. A
5. C

References

1. Aggarwal CC. An introduction to neural networks. In: Aggarwal CC, editor. Neural networks and deep learning: a textbook. Cham: Springer International Publishing; 2018. p. 1–52.
2. Allen T. Particle size measurement. Springer; 2013.
3. Arvaniti E, Claassen M. Sensitive detection of rare disease-associated cell subsets via representation learning. Nat Commun. 2017;8:14825. https://doi.org/10.1038/ncomms14825.
4. Au AK, Lai H, Utela BR, Folch A. Microvalves and micropumps for BioMEMS. Micromachines. 2011;2:179–220. https://doi.org/10.3390/mi2020179.
5. Basiji DA. Principles of amnis imaging flow cytometry. In: Barteneva NS, Vorobjev IA, editors. Imaging flow cytometry: methods and protocols. New York: Springer; 2016. p. 13–21.
6. Basiji DA, Ortyn WE, Liang L, et al. Cellular image analysis and imaging by flow cytometry. Clin Lab Med. 2007;27:653–670, viii. https://doi.org/10.1016/j.cll.2007.05.008
7. Başţanlar Y, Özuysal M. Introduction to machine learning. In: Yousef M, Allmer J, editors. miRNomics: MicroRNA biology and computational analysis. Totowa: Humana Press; 2014. p. 105–28.
8. Bhagat AAS, Kuntaegowdanahalli SS, Kaval N, et al. Inertial microfluidics for sheathless high-throughput flow cytometry. Biomed Microdevices. 2010;12:187–95. https://doi.org/10.1007/s10544-009-9374-9.
9. Burke JM, Zubajlo RE, Smela E, White IM. High-throughput particle separation and concentration using spiral inertial filtration. Biomicrofluidics. 2014;8:024105. https://doi.org/10.1063/1.4870399.
10. Camou S, Fujita H, Fujii T. PDMS 2D optical lens integrated with microfluidic channels: principle and characterization. Lab Chip. 2003;3:40–5. https://doi.org/10.1039/B211280A.
11. Chen J, Zheng Y, Tan Q, et al. Classification of cell types using a microfluidic device for mechanical and electrical measurement on single cells. Lab Chip. 2011;11:3174–81. https://doi.org/10.1039/C1LC20473D.
12. Chia BT, Liao H-H, Yang Y-J. A novel thermo-pneumatic peristaltic micropump with low temperature elevation on working fluid. Sens Actuators Phys. 2011;165:86–93. https://doi.org/10.1016/j.sna.2010.02.018.
13. Choi Y-S, Seo K-W, Lee S-J. Lateral and cross-lateral focusing of spherical particles in a square microchannel. Lab Chip. 2011;11:460–5. https://doi.org/10.1039/C0LC00212G.
14. Di Carlo D, Lee L. Dynamic single-cell analysis for quantitative biology. Anal Chem. 2007;78:7918–25. https://doi.org/10.1021/ac069490p.
15. Diebold ED, Buckley BW, Gossett DR, Jalali B. Digitally synthesized beat frequency multiplexing for sub-millisecond fluorescence microscopy. Nat Photonics. 2013;7:806–10. https://doi.org/10.1038/nphoton.2013.245.
16. Dittrich W, Göhde W. Impulse fluorometry of single cells in suspension. Z Naturforsch B. 1969;24:360–1.
17. Doan M, Carpenter AE. Leveraging machine vision in cell-based diagnostics to do more with less. Nat Mater. 2019;18:414–8. https://doi.org/10.1038/s41563-019-0339-y.

18. Doan M, Case M, Masic D, et al. Label-free leukemia monitoring by computer vision. Cytometry A. 2020a;97:407–14. https://doi.org/10.1002/cyto.a.23987.
19. Doan M, Sebastian JA, Caicedo JC, et al. Objective assessment of stored blood quality by deep learning. Proc Natl Acad Sci USA. 2020b;117:21381–90. https://doi.org/10.1073/pnas.2001227117.
20. Eulenberg P, Köhler N, Blasi T, et al. Reconstructing cell cycle and disease progression using deep learning. Nat Commun. 2017;8:463. https://doi.org/10.1038/s41467-017-00623-3.
21. Foudeh AM, Didar TF, Veres T, Tabrizian M. Microfluidic designs and techniques using lab-on-a-chip devices for pathogen detection for point-of-care diagnostics. Lab Chip. 2012;12:3249–66. https://doi.org/10.1039/C2LC40630F.
22. Gawad S, Cheung K, Seger U, et al. Dielectric spectroscopy in a micromachined flow cytometer: theoretical and practical considerations. Lab Chip. 2004;4:241–51. https://doi.org/10.1039/B313761A.
23. Givan AL. Flow cytometry: an introduction. In: Hawley TS, Hawley RG, editors. Flow cytometry protocols. Totowa: Humana Press; 2011. p. 1–29.
24. Goda K, Ayazi A, Gossett DR, et al. High-throughput single-microparticle imaging flow analyzer. Proc Natl Acad Sci USA. 2012;109:11630–5. https://doi.org/10.1073/pnas.1204718109.
25. Goda K, Tsia KK, Jalali B. Serial time-encoded amplified imaging for real-time observation of fast dynamic phenomena. Nature. 2009;458:1145–9. https://doi.org/10.1038/nature07980.
26. Golden JP, Justin GA, Nasir M, Ligler FS. Hydrodynamic focusing—a versatile tool. Anal Bioanal Chem. 2012;402:325–35. https://doi.org/10.1007/s00216-011-5415-3.
27. Golden JP, Kim JS, Erickson JS, et al. Multi-wavelength microflow cytometer using groove-generated sheath flow. Lab Chip. 2009;9:1942–50. https://doi.org/10.1039/B822442K.
28. Gong Y, Fan N, Yang X, et al. New advances in microfluidic flow cytometry. Electrophoresis. 2019;40:1212–29. https://doi.org/10.1002/elps.201800298.
29. Gou Y, Jia Y, Wang P, Sun C. Progress of inertial microfluidics in principle and application. Sensors. 2018;18:1762. https://doi.org/10.3390/s18061762.
30. Gross HJ, Verwer B, Houck D, Recktenwald D. Detection of rare cells at a frequency of one per million by flow cytometry. Cytometry. 1993;14:519–26. https://doi.org/10.1002/cyto.990140511.
31. Gu W, Chen H, Tung Y-C, et al. Multiplexed hydraulic valve actuation using ionic liquid filled soft channels and braille displays. Appl Phys Lett. 2007;90:033505. https://doi.org/10.1063/1.2431771.
32. Göröcs Z, Tamamitsu M, Bianco V, et al. A deep learning-enabled portable imaging flow cytometer for cost-effective, high-throughput, and label-free analysis of natural water samples. Light Sci Appl. 2018;7:66. https://doi.org/10.1038/s41377-018-0067-0.
33. Han Y, Lo Y-H. Imaging cells in flow cytometer using spatial-temporal transformation. Sci Rep. 2015;5:13267. https://doi.org/10.1038/srep13267.
34. Han Y, Tang R, Gu Y, et al. Cameraless high-throughput three-dimensional imaging flow cytometry. Optica. 2019;6:1297–304. https://doi.org/10.1364/OPTICA.6.001297.
35. Hasegawa D, Bugarin C, Giordan M, et al. Validation of flow cytometric phospho-STAT5 as a diagnostic tool for juvenile myelomonocytic leukemia. Blood Cancer J. 2013;3:e160. https://doi.org/10.1038/bcj.2013.56.
36. He T, Li X. Image quality recognition technology based on deep learning. J Vis Commun Image Represent. 2019;65:102654. https://doi.org/10.1016/j.jvcir.2019.102654.
37. Hengoju S, Shvydkiv O, Tovar M, et al. Advantages of optical fibers for facile and enhanced detection in droplet microfluidics. Biosens Bioelectron. 2022;200:113910. https://doi.org/10.1016/j.bios.2021.113910.
38. Herzenberg LA, Parks D, Sahaf B, et al. The history and future of the fluorescence activated cell sorter and flow cytometry: a view from Stanford. Clin Chem. 2002;48:1819–27.
39. Holmes D, Morgan H. Single cell impedance cytometry for identification and counting of CD4 T-cells in human blood using impedance labels. Anal Chem. 2010;82:1455–61. https://doi.org/10.1021/ac902568p.

40. Holzner G, Du Y, Cao X, et al. An optofluidic system with integrated microlens arrays for parallel imaging flow cytometry. Lab Chip. 2018;18:3631–7. https://doi.org/10.1039/C8LC00593A.
41. Holzner G, Mateescu B, Van Leeuwen D, et al. High-throughput multiparametric imaging flow cytometry: toward diffraction-limited sub-cellular detection and monitoring of sub-cellular processes. Cell Rep. 2021;34:108824. https://doi.org/10.1016/j.celrep.2021.108824.
42. Holzner G, Stavrakis S, deMello A. Elasto-inertial focusing of mammalian cells and bacteria using low molecular, low viscosity PEO solutions. Anal Chem. 2017;89:11653–63. https://doi.org/10.1021/acs.analchem.7b03093.
43. Hoogendoorn KH. Advanced therapies: clinical, non-clinical and quality considerations. In: Crommelin DJA, Sindelar RD, Meibohm B, editors. Pharmaceutical biotechnology: fundamentals and applications. Cham: Springer International Publishing; 2019. p. 357–402.
44. Hou L, Samaras D, Kurc TM, et al. Patch-based convolutional neural network for whole slide tissue image classification. 2016. p. 2424–33.
45. Huang F, Sirinakis G, Allgeyer ES, et al. Ultra-high resolution 3D imaging of whole cells. Cell. 2016;166:1028–40. https://doi.org/10.1016/j.cell.2016.06.016.
46. Hur SC, Tse HTK, Carlo DD. Sheathless inertial cell ordering for extreme throughput flow cytometry. Lab Chip. 2010;10:274–80. https://doi.org/10.1039/B919495A.
47. Isozaki A, Mikami H, Tezuka H, et al. Intelligent image-activated cell sorting 2.0. Lab Chip. 2020;20:2263–73. https://doi.org/10.1039/D0LC00080A.
48. Janowczyk A, Madabhushi A. Deep learning for digital pathology image analysis: a comprehensive tutorial with selected use cases. J Pathol Inform. 2016;7:29. https://doi.org/10.4103/2153-3539.186902.
49. Jiang H, Weng X, Li D. Dual-wavelength fluorescent detection of particles on a novel microfluidic chip. Lab Chip. 2013;13:843–50. https://doi.org/10.1039/C2LC41238A.
50. Jiang Y, Lei C, Yasumoto A, et al. Label-free detection of aggregated platelets in blood by machine-learning-aided optofluidic time-stretch microscopy. Lab Chip. 2017;17:2426–34. https://doi.org/10.1039/C7LC00396J.
51. Kamentsky LA, Melamed MR, Derman H. Spectrophotometer: new instrument for ultrarapid cell analysis. Science. 1965;150:630–1. https://doi.org/10.1126/science.150.3696.630.
52. Karen C, Gawad S, Renaud P. Impedance spectroscopy flow cytometry: on-chip label-free cell differentiation. Cytom Part J Int Soc Anal Cytol. 2005;65:124–32. https://doi.org/10.1002/cyto.a.20141.
53. Kim J, Lee J, Wu C, et al. Inertial focusing in non-rectangular cross-section microchannels and manipulation of accessible focusing positions. Lab Chip. 2016;16:992–1001. https://doi.org/10.1039/C5LC01100K.
54. Kim J, Lee J-R, Je T-J, et al. Size-dependent inertial focusing position shift and particle separations in triangular microchannels. Anal Chem. 2018;90:1827–35. https://doi.org/10.1021/acs.analchem.7b03851.
55. Kourou K, Exarchos TP, Exarchos KP, et al. Machine learning applications in cancer prognosis and prediction. Comput Struct Biotechnol J. 2015;13:8–17. https://doi.org/10.1016/j.csbj.2014.11.005.
56. Lai QTK, Lee KCM, Tang AHL, et al. High-throughput time-stretch imaging flow cytometry for multi-class classification of phytoplankton. Opt Express. 2016;24:28170–84. https://doi.org/10.1364/OE.24.028170.
57. Lee MG, Choi S, Park J-K. Three-dimensional hydrodynamic focusing with a single sheath flow in a single-layer microfluidic device. Lab Chip. 2009;9:3155–60. https://doi.org/10.1039/B910712F.
58. Li D, Lu X, Xuan X. Viscoelastic separation of particles by size in straight rectangular microchannels: a parametric study for a refined understanding. Anal Chem. 2016;88:12303–9. https://doi.org/10.1021/acs.analchem.6b03501.
59. Lim EJ, Ober TJ, Edd JF, et al. Inertio-elastic focusing of bioparticles in microchannels at high throughput. Nat Commun. 2014;5:4120. https://doi.org/10.1038/ncomms5120.

60. Lippeveld M, Knill C, Ladlow E, et al. Classification of human white blood cells using machine learning for stain-free imaging flow cytometry. Cytometry A. 2020;97:308–19. https://doi.org/10.1002/cyto.a.23920.
61. Lugli E, Roederer M, Cossarizza A. Data analysis in flow cytometry: the future just started. Cytom Part J Int Soc Anal Cytol. 2010;77:705–13. https://doi.org/10.1002/cyto.a.20901.
62. Luo S, Shi Y, Chin LK, et al. Machine-learning-assisted intelligent imaging flow cytometry: a review. Adv Intell Syst. 2021;3:2100073. https://doi.org/10.1002/aisy.202100073.
63. Macey MG. Principles of flow cytometry. In: Macey MG, editor. Flow cytometry: principles and applications. Totowa: Humana Press; 2007. p. 1–15.
64. Mao X, Lin S-CS, Dong C, Huang TJ. Single-layer planar on-chip flow cytometer using microfluidic drifting based three-dimensional (3D) hydrodynamic focusing. Lab Chip. 2009;9:1583–9. https://doi.org/10.1039/B820138B.
65. Mao X, Nawaz AA, Lin S-CS, et al. An integrated, multiparametric flow cytometry chip using "microfluidic drifting" based three-dimensional hydrodynamic focusing. Biomicrofluidics. 2012;6:024113. https://doi.org/10.1063/1.3701566.
66. Maramorosch K. Tissue culture: methods and applications by Paul F. Kruse, Jr., M. K. Patterson, Jr. J N Y Entomol Soc. 1974;82:201.
67. Matsumura H, Tzu-Wei Shen L, Isozaki A, et al. Virtual-freezing fluorescence imaging flow cytometry with 5-aminolevulinic acid stimulation and antibody labeling for detecting all forms of circulating tumor cells. Lab Chip. 2023;23:1561–75. https://doi.org/10.1039/D2LC00856D.
68. Meng N, Lam EY, Tsia KK, So HK-H. Large-scale multi-class image-based cell classification with deep learning. IEEE J Biomed Health Inform. 2019;23:2091–8. https://doi.org/10.1109/JBHI.2018.2878878.
69. Mikami H, Gao L, Goda K. Ultrafast optical imaging technology: principles and applications of emerging methods. Nano. 2016;5:497–509. https://doi.org/10.1515/nanoph-2016-0026.
70. Mikami H, Harmon J, Kobayashi H, et al. Ultrafast confocal fluorescence microscopy beyond the fluorescence lifetime limit. Optica. 2018;5:117–26. https://doi.org/10.1364/OPTICA.5.000117.
71. Mikami H, Kawaguchi M, Huang C-J, et al. Virtual-freezing fluorescence imaging flow cytometry. Nat Commun. 2020;11:1162. https://doi.org/10.1038/s41467-020-14929-2.
72. Min X, Kim WS. Beyond high voltage in the digital microfluidic devices for an integrated portable sensing system. Microfluid Nanofluidics. 2019;23:127. https://doi.org/10.1007/s10404-019-2294-y.
73. Miura T, Mikami H, Isozaki A, et al. On-chip light-sheet fluorescence imaging flow cytometry at a high flow speed of 1 m/s. Biomed Opt Express. 2018;9:3424–33. https://doi.org/10.1364/BOE.9.003424.
74. Nassar M, Doan M, Filby A, et al. Label-free identification of white blood cells using machine learning. Cytometry A. 2019;95:836–42. https://doi.org/10.1002/cyto.a.23794.
75. Nebe-von-Caron G, Stephens PJ, Hewitt CJ, et al. Analysis of bacterial function by multi-colour fluorescence flow cytometry and single cell sorting. J Microbiol Methods. 2000;42:97–114. https://doi.org/10.1016/s0167-7012(00)00181-0.
76. Nitta N, Sugimura T, Isozaki A, et al. Intelligent image-activated cell sorting. Cell. 2018;175:266–276.e13. https://doi.org/10.1016/j.cell.2018.08.028.
77. Nolan JP, Duggan E. Analysis of individual extracellular vesicles by flow cytometry. Methods Mol Biol. 2018;1678:79–92. https://doi.org/10.1007/978-1-4939-7346-0_5.
78. Otesteanu CF, Ugrinic M, Holzner G, et al. A weakly supervised deep learning approach for label-free imaging flow-cytometry-based blood diagnostics. Cell Rep Methods. 2021;1:100094. https://doi.org/10.1016/j.crmeth.2021.100094.
79. Ozkumur E, Shah AM, Ciciliano JC, et al. Inertial focusing for tumor antigen-dependent and -independent sorting of rare circulating tumor cells. Sci Transl Med. 2013;5:179ra47. https://doi.org/10.1126/scitranslmed.3005616.

80. Paiè P, Bragheri F, Di Carlo D, Osellame R. Particle focusing by 3D inertial microfluidics. Microsyst Nanoeng. 2017;3:1–8. https://doi.org/10.1038/micronano.2017.27.
81. Perfetto SP, Chattopadhyay PK, Roederer M. Seventeen-colour flow cytometry: unravelling the immune system. Nat Rev Immunol. 2004;4:648–55. https://doi.org/10.1038/nri1416.
82. Pischel D, Buchbinder JH, Sundmacher K, et al. A guide to automated apoptosis detection: how to make sense of imaging flow cytometry data. PLoS One. 2018;13:e0197208. https://doi.org/10.1371/journal.pone.0197208.
83. Piyasena ME, Graves SW. The intersection of flow cytometry with microfluidics and microfabrication. Lab Chip. 2014;14:1044–59. https://doi.org/10.1039/C3LC51152A.
84. Qiu P, Simonds EF, Bendall SC, et al. Extracting a cellular hierarchy from high-dimensional cytometry data with SPADE. Nat Biotechnol. 2011;29:886–91. https://doi.org/10.1038/nbt.1991.
85. Rane AS, Rutkauskaite J, deMello A, Stavrakis S. High-throughput multi-parametric imaging flow cytometry. Chem. 2017;3:588–602. https://doi.org/10.1016/j.chempr.2017.08.005.
86. Regmi R, Mohan K, Mondal PP. High resolution light-sheet based high-throughput imaging cytometry system enables visualization of intra-cellular organelles. AIP Adv. 2014;4:097125. https://doi.org/10.1063/1.4896260.
87. Rodríguez-Ruiz I, Ackermann TN, Muñoz-Berbel X, Llobera A. Photonic Lab-on-a-Chip: integration of optical spectroscopy in microfluidic systems. Anal Chem. 2016;88:6630–7. https://doi.org/10.1021/acs.analchem.6b00377.
88. Rosa S, Herzenberg L, Roederer M. 11-color, 13-parameter flow cytometry: identification of human naive T cells by phenotype, function, and T-cell receptor diversity. Nat Med. 2001;7:245–8. https://doi.org/10.1038/84701.
89. Rubin M, Stein O, Turko NA, et al. TOP-GAN: stain-free cancer cell classification using deep learning with a small training set. Med Image Anal. 2019;57:176–85. https://doi.org/10.1016/j.media.2019.06.014.
90. Sackmann EK, Fulton AL, Beebe DJ. The present and future role of microfluidics in biomedical research. Nature. 2014;507:181–9. https://doi.org/10.1038/nature13118.
91. Salmanzadeh A, Shafiee H, Davalos RV, Stremler MA. Microfluidic mixing using contactless dielectrophoresis. Electrophoresis. 2011;32:2569–78. https://doi.org/10.1002/elps.201100171.
92. Schafer D, Gibson EA, Salim EA, et al. Microfluidic cell counter with embedded optical fibers fabricated by femtosecond laser ablation and anodic bonding. Opt Express. 2009;17:6068–73. https://doi.org/10.1364/OE.17.006068.
93. Scheau C, Didilescu AC, Caruntu C. Medical application of functional biomaterials—the future is now. J Funct Biomater. 2022;13:244. https://doi.org/10.3390/jfb13040244.
94. Schonbrun E, Gorthi SS, Schaak D. Microfabricated multiple field of view imaging flow cytometry. Lab Chip. 2011;12:268–73. https://doi.org/10.1039/C1LC20843H.
95. Shapiro. Practical flow cytometry. 1st ed. John Wiley & Sons, Ltd; 2003.
96. Shi W, Guo L, Kasdan H, Tai Y-C. Four-part leukocyte differential count based on sheathless microflow cytometer and fluorescent dye assay. Lab Chip. 2013;13:1257–65. https://doi.org/10.1039/C3LC41059E.
97. Simon P, Frankowski M, Bock N, Neukammer J. Label-free whole blood cell differentiation based on multiple frequency AC impedance and light scattering analysis in a micro flow cytometer. Lab Chip. 2016;16:2326–38. https://doi.org/10.1039/c6lc00128a.
98. Stavrakis S, Holzner G, Choo J, deMello A. High-throughput microfluidic imaging flow cytometry. Curr Opin Biotechnol. 2019;55:36–43. https://doi.org/10.1016/j.copbio.2018.08.002.
99. Stelzer EHK. Light-sheet fluorescence microscopy for quantitative biology. Nat Methods. 2015;12:23–6. https://doi.org/10.1038/nmeth.3219.
100. Stone HA, Stroock AD, Ajdari A. Engineering flows in small devices: microfluidics toward a Lab-on-a-Chip. Annu Rev Fluid Mech. 2004;36:381–411. https://doi.org/10.1146/annurev.fluid.36.050802.122124.

101. Telford WG. Overview of lasers for flow cytometry. In: Hawley TS, Hawley RG, editors. Flow cytometry protocols. New York: Springer; 2018. p. 447–79.
102. Toner M, Irimia D. Blood-on-a-chip. Annu Rev Biomed Eng. 2005;7:77–103. https://doi.org/10.1146/annurev.bioeng.7.011205.135108.
103. Ugawa M, Ota S. High-throughput parallel optofluidic 3D-imaging flow cytometry. Small Sci. 2022;2:2100126. https://doi.org/10.1002/smsc.202100126.
104. Vembadi A, Menachery A, Qasaimeh MA. Cell cytometry: review and perspective on biotechnological advances. Front Bioeng Biotechnol. 2019;7:147.
105. Wang X, Gao H, Dindic N, et al. A low-cost, plug-and-play inertial microfluidic helical capillary device for high-throughput flow cytometry. Biomicrofluidics. 2017;11:014107. https://doi.org/10.1063/1.4974903.
106. Whitesides GM. The origins and the future of microfluidics. Nature. 2006;442:368–73. https://doi.org/10.1038/nature05058.
107. Wong TTW, Lau AKS, Ho KKY, et al. Asymmetric-detection time-stretch optical microscopy (ATOM) for ultrafast high-contrast cellular imaging in flow. Sci Rep. 2014;4:3656. https://doi.org/10.1038/srep03656.
108. Xia Y, Whitesides GM. Soft lithography. Angew Chem Int Ed Engl. 1998;37:550–75. https://doi.org/10.1002/(SICI)1521-3773(19980316)37:5<550::AID-ANIE550>3.0.CO;2-G.
109. Xiang N, Ni Z, Yi H. Concentration-controlled particle focusing in spiral elasto-inertial microfluidic devices. Electrophoresis. 2018;39:417–24. https://doi.org/10.1002/elps.201700150.
110. Xiang N, Zhang X, Dai Q, et al. Fundamentals of elasto-inertial particle focusing in curved microfluidic channels. Lab Chip. 2016;16:2626–35. https://doi.org/10.1039/C6LC00376A.
111. Xun W, Feng J, Chang H. A microflow cytometer based on a disposable microfluidic chip with side scatter and fluorescence detection capability. IEEE Trans Nanobioscience. 2015;14:850–6. https://doi.org/10.1109/TNB.2015.2455073.
112. Yang R-J, Fu L-M, Hou H-H. Review and perspectives on microfluidic flow cytometers. Sens Actuators B Chem. 2018;266:26. https://doi.org/10.1016/j.snb.2018.03.091.
113. Yang S, Kim JY, Lee SJ, et al. Sheathless elasto-inertial particle focusing and continuous separation in a straight rectangular microchannel. Lab Chip. 2011;11:266–73. https://doi.org/10.1039/C0LC00102C.
114. Yang SH, Lee DJ, Youn JR, Song YS. Multiple-line particle focusing under viscoelastic flow in a microfluidic device. Anal Chem. 2017;89:3639–47. https://doi.org/10.1021/acs.analchem.6b05052.
115. Yaralioglu GG, Wygant IO, Marentis TC, Khuri-Yakub BT. Ultrasonic mixing in microfluidic channels using integrated transducers. Anal Chem. 2004;76:3694–8. https://doi.org/10.1021/ac035220k.
116. Yuan D, Zhao Q, Yan S, et al. Recent progress of particle migration in viscoelastic fluids. Lab Chip. 2018;18:551–67. https://doi.org/10.1039/C7LC01076A.
117. Zhao Y, Liu Q, Sun H, et al. Electrical property characterization of neural stem cells in differentiation. PLoS One. 2016;11:e0158044. https://doi.org/10.1371/journal.pone.0158044.
118. Zhu S, Zhang X, Zhou Z, et al. Microfluidic impedance cytometry for single-cell sensing: review on electrode configurations. Talanta. 2021;233:122571. https://doi.org/10.1016/j.talanta.2021.122571.
119. Fan YJ, Wu YC, Chen Y, Kung YC, Wu TH, Huang KW, Sheen HJ, Chiou PY. Three dimensional microfluidics with embedded microball lenses for parallel and high throughput multicolor fluorescence detection. Biomicrofluidics. 2013;7(4):44121. https://doi.org/10.1063/1.4818944. PMID: 24404054